PROCEEDINGS OF SPIE

SPIEDigitalLibrary.org/conference-proceedings-of-spie

15 focal planes head-mounted display using LED array backlight

Dongheon Yoo, Seungjae Lee, Youngjin Jo, Jaebum Cho, Suyeon Choi, et al.

Dongheon Yoo, Seungjae Lee, Youngjin Jo, Jaebum Cho, Suyeon Choi, Byoungho Lee, "15 focal planes head-mounted display using LED array backlight," Proc. SPIE 11040, Optical Design Challenge 2019, 110400D (27 February 2019); doi: 10.1117/12.2525055

SPIE.

Event: SPIE Optical Design Challenge, 2019, San Francisco, California, United States

15 Focal Planes Head-Mounted Display using LED Array Backlight

Dongheon Yoo† , Seungjae Lee† , Youngjin Jo, Jaebum Cho, Suyeon Choi , and Byoungho Lee*

School of Electrical and Computer Engineering, Seoul National University, Gwanak-Gu Gwanakro 1, Seoul 08826, South Korea

ABSTRACT

Currently, commercial head-mounted displays suffer from limited accommodative states, which lead to vergence-accommodation conflict. In this work, we newly design the architecture of head-mounted display supporting 15 focal planes over wide depth of field (20cm-optical infinity) in real time to alleviate vergence-accommodation conflict. Our system employs a low-resolution vertical scanning backlight, a display panel (e.g. liquid crystal panel), and focus-tunable lens. We demonstrate the compact prototype and verify its performance through experimental results.

Keywords: Head-mounted display, Vergence-accommodation conflict, Virtual reality, Volumetric display

1. INTRODUCTION

Virtual reality is an emerging technology considered as one of the most promising next-generation displays. Virtual reality has large potential to be applied in several fields including education, medical assistants, simulation training, and entertainments. Increased interest of the public in virtual reality involves the rapid development of head-mounted displays (HMDs). HMDs are recognized as feasible and efficient platform to deliver immersive visual experience via stereoscopic imagery. HMDs for virtual reality have already been penetrating to our daily life where we can easily experience 3D entertainment using commercialized HMD products. Although state-of-the-art HMDs may provide large field of view ($\geq 90°$) or high resolution (UHD), the specifications are still insufficient to satisfy the users demand. Especially, it is challenging to resolve vergence-accommodation conflict (VAC) caused by the mismatch between the focal depths of virtual objects and the display plane. VAC could raise several artifacts and visual fatigue including double vision, nausea, and dizziness.[1–3]

In order to alleviate VAC, we may utilize volumetric displays that generate multiple focal planes to provide users with accommodation cues. Volumetric displays may support continuous focus cues via merging focal plane images. For continuous and accurate focus cues, it is important to determine appropriate spacing between adjacent focal planes. Rolland et al.[4] reported that 14 focal planes are required to deliver high quality images of 20 cycle per degree (cpd) within 2.0 diopter (D) depth range. Although Mackenzie et al.[5] verified that much less focal planes of larger spacing (0.6D−1.0D) is enough to induce natural focus cues, the resolution of retinal images is traded for focus cues. Thus, the number of focal planes is a key factor to determine display performance of volumetric displays in terms of resolution, depth of field, and focus cue accuracy.

Volumetric displays employ temporal[6,7] or spatial[8] multiplexing method to generate focal planes. However, it has been a challenging goal to achieve large number of focal planes without the loss of frame rate or resolution. Here, we introduce a novel method that relieves the trade-off relationship among the number of focal planes, frame rate, resolution, and depth of field. Synchronizing a focus-tunable lens and a light emitting diode (LED) array backlight, our method generates 15 focal planes over the extended depth of field (20cm-optical infinity) that can be refreshed at 60 frames per second (fps). The most significant contribution of our work is implementation of compact and practical head-mounted display system with focus cues. Our prototype consists of off-the-shelf components, demands relatively less computation load, and has large potential to enhance display performance such as field of view, resolution, and eye-box.

†The first two authors equally contributed.

*Byoungho Lee is the corresponding author. (e-mail: byoungho@snu.ac.kr)

Optical Design Challenge 2019, edited by Bernard C. Kress, Christophe Peroz, Proc. of SPIE
Vol. 11040, 110400D · © 2019 SPIE · CCC code: 0277-786X/19/$18 · doi: 10.1117/12.2525055

In this study, we will explore the optical principle of proposed system and low-level methodologies to resolve several issues related to the system. First, we introduce our previous work using a digital micromirror device (DMD)[9] instead of the LED array. The brief description of the previous research would give intuition to understand the advantages and limitations of the LED array backlight. Second, we will demonstrate and discuss approaches to overcome the refresh rates of the LED array backlight and the limited resolution. Third, we conclude with experimental results of implemented prototype, which shows feasibility and validity of our methods.

2. RELATED WORK

2.1 Light-field and Holographic Displays

Light-field displays aim to reconstruct four-dimensional light-field that passes through the eye-box. Various approaches have been introduced including integral imaging,[10] multi-view,[11] and multi-layered displays[12–15] in order to modulate angular direction of light field. Although these methods have distinct optical principles and structures, they have a common limitation involved by the trade-off between the spatial and angular resolution. Since light-field is defined by four independent variables, reconstruction of light-field requires mass amount of information. However, display panel has a limited number of pixels to represent light-field with degradation in spatial resolution.

Holographic displays are considered as one of the feasible solutions to overcome the limitation of light-field displays. As holographic displays reconstruct a complex wavefront from a volumetric object rather than light field, they are relatively free from the trade-off between spatial and angular resolution. Recently, holographic displays have been thoroughly explored for application in HMDs. Various optical structures using a wave guide,[16] a holographic image combiner,[17] or a beam steering element[18] were introduced to improve the form factor, field of view, or eye-box. However, it is still challenging to implement holographic HMDs with large field of view and eye-box due to the limited bandwidth of spatial light modulators. In addition, speckle noise as well as large computational demand are barriers for commercialization of holographic displays.

2.2 Volumetric Displays

Volumetric displays (or multi-plane displays) reconstruct discrete focal planes to provide users with depth information. Compared to light-field and holographic displays, volumetric displays focus on immersive and comfort experience of users. Precise reconstruction of light-field or wavefront is not primary factor to determine focal plane images or optical structures. Volumetric displays determine these optical specifications in consideration of the accommodation depth and retinal image fidelity. For instance, various algorithms[19–21] to optimize retinal images were introduced for volumetric displays, which allow users to have more immersive experience by covering accurate blur or occlusion effect. As a result, volumetric displays have superior display performance including spatial resolution, field of view, and exit-pupil.

Despite of the advantages, volumetric displays have been considered as an impractical approach for HMDs. Volumetric displays suffer from the narrow depth of field involved by limited number of focal planes. It has been challenging to increase the number of focal planes without scarification of frame rate or resolution. State-of-the-art prototype using a DMD projection system[22] may form 24-bit color images at 11 focal planes. To our knowledge, however, the effective number of focal planes is reduced to 6 if we consider motion blur which is discussed in the Section 3.2. In addition, the DMD projection system inhibits the compact optical design of HMDs.

2.3 Tomographic Displays

Tomographic displays[9] reconstruct multiple focal plane images by updating backlight images rather than display images. While the focal plane depth is modulated by a focus-tunable lens, display pixels are selectively illuminated by backlight so that each pixel is floated at the desired depth. As backlight is updated via binary modulation, the refresh rate could be much faster than ordinary display panels. In other words, tomographic displays may have large number of focal planes by using off-the-shelf components. In a previous work, we introduced a near-eye display system with 80 focal planes using a DMD projection system. Here, we demonstrate a wearable display system with 15 focal planes using a LED array instead of the DMD. It is a significant breakthrough to realize practical and efficient HMDs with focus cues.

3. TOMOGRAPHIC HEAD-MOUNTED DISPLAYS

3.1 Design

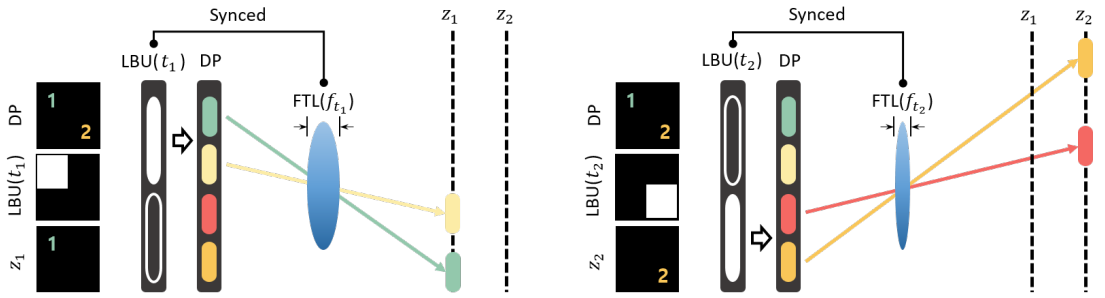

Figure 1. Simplified diagram describing working principle of tomographic HMDs.

Our design is composed of focus-tunable lenses (FTLs), display panel (DP) and low-resolution backlight unit (LBU). LBU consists of commercial LED array and optical diffuser to increase the fill factor of LED pixel. Figure 1 describes how these optical components float images on different focal planes. For simplicity, we suppose the monocular case. The FTL operates at a speed of 60Hz and its focal length continuously changes during this period. It is driven by external voltage signal and it sweeps from 20cm (5.0D) to optical infinity (0.0D), which decides the depth range of our system. When FTL generates the focal plane on the distance of z_1, partial image (1 of green color) of DP is illuminated by LBU. In the same way, partial image (2 of yellow color) of DP is illuminated when FTL forms an image on z_2. The FTL and LBU should be synchronized precisely in order to synthesize three-dimensional scenes with correct depth value. During a single frame (16.66ms), LBU is modulated for 15 times and DP shows static two-dimensional images so that frame rates of components would be 900Hz and 60Hz, respectively.

3.2 Increasing the number of focal planes

In this section, we demonstrate an operating strategy of the LED array backlight that updates binary images. The primary goal of the operation strategy is to maximize the refresh rates of the LED array backlight for denser focal plane reconstruction. Applying the operation strategy, we may drive a commercially available LED array (RGB LED Matrix from Adafruit) at the fast frame rate of 900Hz so that tomographic displays reconstruct the 15 focal planes. In other words, the proposed operation method could resolve the limited refresh rate of the LED array compared to a DMD projection system. In addition, the operation strategy minimizes various artifacts including flickering effect and depth distortion.

In advance of the description of the LED array operation strategy, we need to understand how LED array updates binary images. Commercial LED arrays, which could be purchased by affordable cost, usually employ the vertical scanning method to determine on/off state of each pixel. Thus, the frame rates of LED arrays are inversely proportional to the number of vertical scanning rows. Exploiting the inverse relationship, the proposed LED array operation strategy may double the frame rates by driving half of LED array. The decline in the vertical resolution of LED array could be compensated by using both of the sweeping direction of the FTL. As shown in the Fig. 2, upper half of LED array is refreshed during the first half period where the focal length of the FTL is getting longer, and lower half of LED arrays is utilized for the second half period. As a result, tomographic displays could have denser focal planes via proposed LED array operation. Furthermore, the proposed operation strategy mitigates the depth discrepancy between the first and the last rows of LED array. We need to minimize the time delay for vertical scanning that may cause depth distortion of reconstructed focal planes.

It is also feasible to double the focal plane number by presenting a slight delay in synchronization of the backlight and the tunable lens.[22] Compared to this primitive method, the proposed operation strategy has several advantages. First, our method is almost free from the flickering effect caused by motion blur since each LED pixel has black frame, as shown in the Fig. 3. White arrows in the Fig. 3 represents black hole artifact caused by the LBU pixel not lighting at that position. Meanwhile, red arrows indicates mixed frames as the

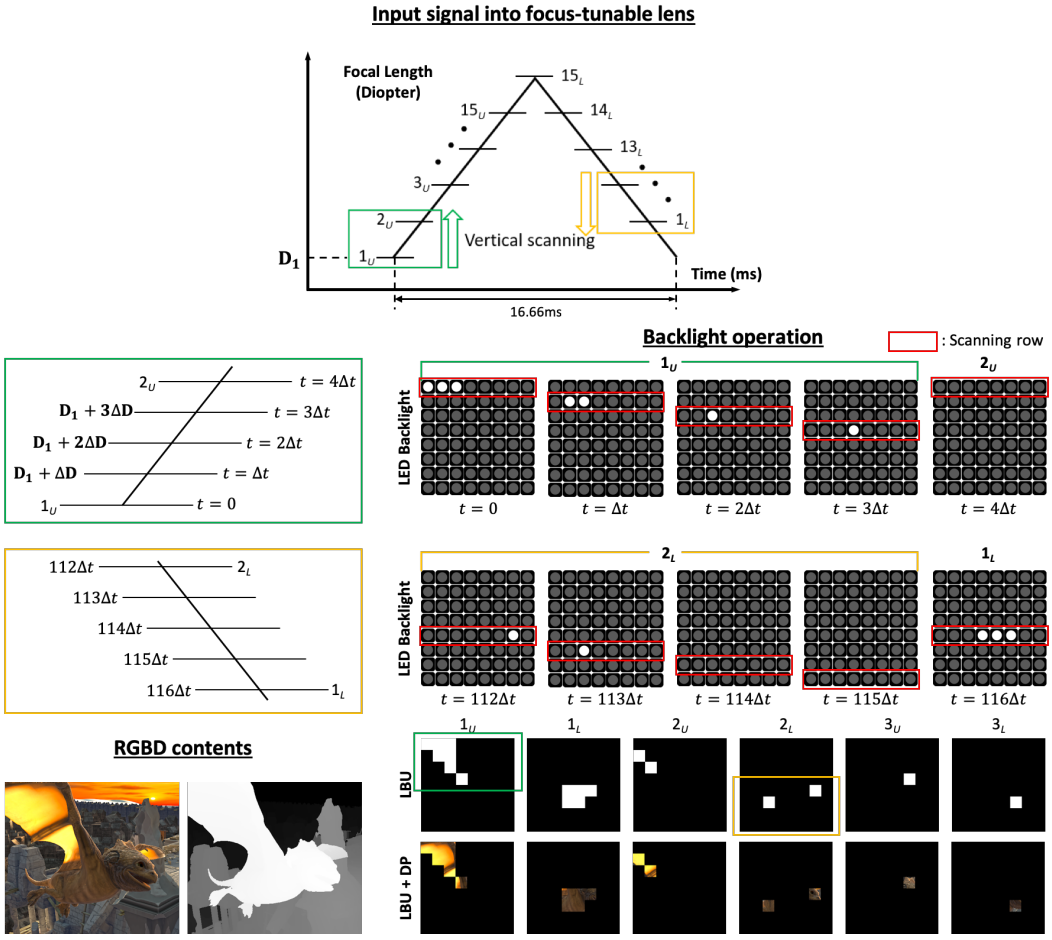

Figure 2. Overview of proposed focal plane allocation strategy. In the top diagram, we illustrate how focal planes are distributed within a single period of FTL oscillation. Horizontal lines with distinct numbers denote the starting points of LBU frames and each frame is vertically scanned in sequence. With our proposed strategy, only upper half area of LBU is turned on in the first half period and the other lower half area in the second half period. For instance, 1_U and 1_L indicate the upper and lower part of 1st focal plane and they are floated in the former and latter half period. Referring to enlarged diagrams (green box and yellow box), our strategy could alleviate depth distortion caused by sequential scanning as well. With respect to the RGBD contents[23] in lower left images, how each LBU frame $(1_U, 1_L, 2_U, 2_L)$ is spatially decomposed over the whole period is shown in the middle images. Several examples of LBU and resultant focal plane images are presented as well.

specific LBU pixel is lit in both frames. It is a significant merit for active display system to allow users to observe a 60fps video without undesired artifacts. Second, the depth discrepancy is reduced by half with our approach as each LBU frame consumes less time ($4\Delta t$ in the Fig. 2) for scanning than conventional approach ($8\Delta t$).

3.3 Low-resolution backlight issues

Although LBU has the advantage of being compact and capable of modulating at a high speed, its resolution is significantly low compared to the DP. In terms of the image quality, the depth value of unit voxel should be carefully determined as it does not correspond to a single pixel of the display panel but the set of a number of pixels. Let us suppose the number of pixels constituting LBU and DP as N_B and N_D, respectively. The two-dimensional image on the DP is split into small N_B image blocks and N_D/N_B pixels on the DP represent single depth value as each block functions as an unit voxel of synthesized scenes. We fit this value by minimizing total retinal blur diameter error as shown in the Fig. 4. According to the work by Chakravarthula et al.,[24]

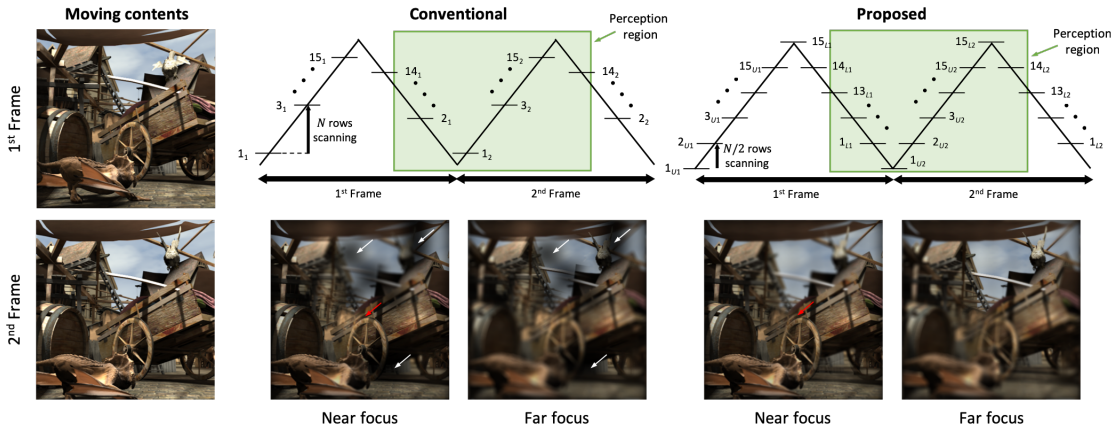

Figure 3. Simulation results for comparison of backlight operation methods with respect to displaying moving scenes.[23] In terms of such scenes, perception period of human eye may vary so that information of consecutive frames is smeared into each other. The perception range is supposed to cover partial periods of the 1st frame and the 2nd frame. If the system uses $N \times N$ pixels of the backlight, each frame sequentially turns on N rows and $N/2$ rows according to conventional approach and proposed approach, respectively. Although conventional mode support the same number of focal planes with proposed mode, synthesized scenes over the region deteriorates since images on the focal planes are distributed over the whole display area. On the other hand, the results for proposed mode are relatively clear since images of the 1st frame are distributed in the lower half area and the 2nd frame in the upper half area.

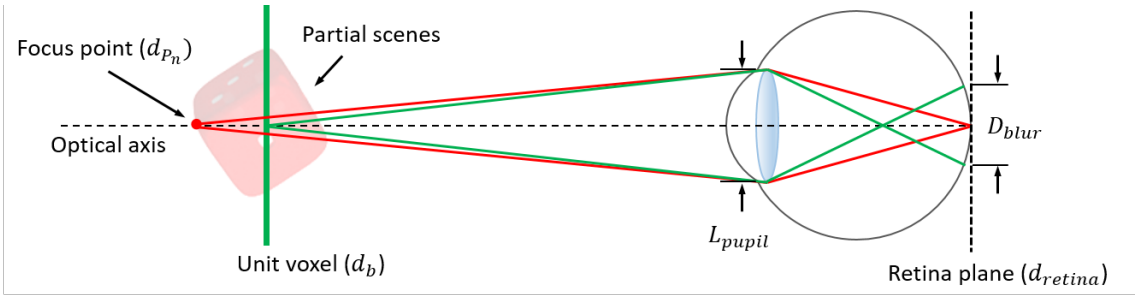

Figure 4. Modeling retinal blur when human eye focuses on the distance of target scene rendered by single pixel in the display panel.[24] Originally, the focus point in the figure should be floated in the d_{P_n} but it is physically floated in the d_b which is the location of unit voxel since entire pixels in the voxel could not have distinct depth states. Therefore, the retinal blur arises as the system error.

perceived retinal blur diameter D_{blur} is defined as

$$D_{blur} = L_{pupil} \frac{|d_b - d_{P_n}|}{d_b} M, \tag{1}$$

where L_{pupil}, d_b, d_{P_n} and M is the pupil diameter of crystalline lens of the eye, distance of floated image block, ground truth depth value of single pixel and magnification by the eye lens, respectively. Originally, each pixel P_n in the block should be floated at distinct distance according to depth map of target scenes. However, the whole pixels in the block are floated at a single focal plane and retinal blur disk arises when the observer accommodates on the distance of d_{P_n}. We define the blur disk diameter as the retinal blur error for single pixel. Magnification M can be derived from simple geometric relationship as

$$M = \frac{d_{retina}}{d_{P_n}}, \tag{2}$$

where d_{retina} is distance of retinal plane. Combining two equations, it could be found that the error is proportional to the difference between d_b and d_{P_n} in dioptric unit since the pupil diameter and retinal plane location are constant. Thus, total error E within the unit voxel could be computed as

$$E = \sum_{n=1}^{N_D/N_B} |\frac{1}{d_{P_n}} - \frac{1}{d_b}|^2. \tag{3}$$

We choose the distance of unit voxel as the mean dioptric depth value of constituting pixels to minimize the error E. Therefore, the resultant dioptric depth value of the voxel $\frac{1}{d_b}$ would be

$$\frac{1}{d_b} = \frac{1}{N_D/N_B} \sum_{n=1}^{N_D/N_B} \frac{1}{d_{P_n}}. \tag{4}$$

4. IMPLEMENTATION AND RESULTS

4.1 Hardware

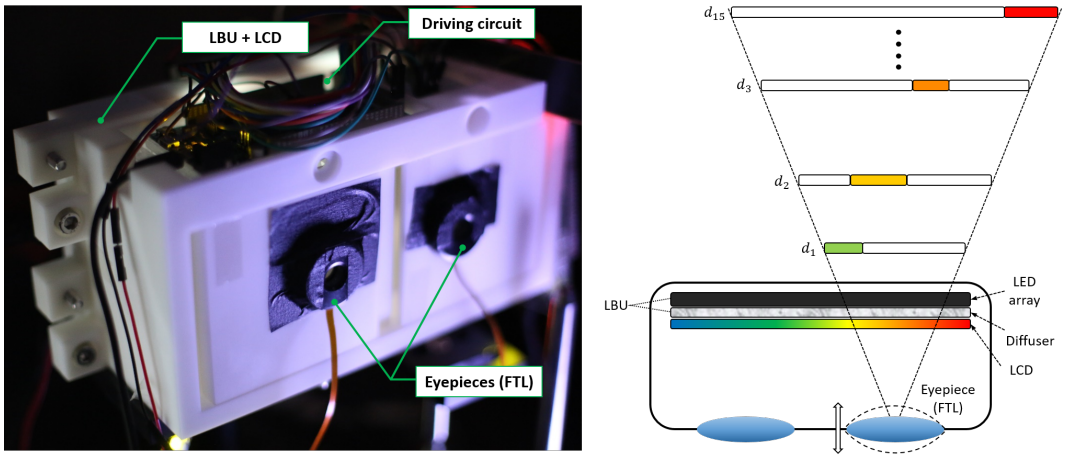

Figure 5. Demonstration of tomographic HMD prototype. On the left side, a photograph of our prototype is presented. Three main components (LBU, DP, FTL) are packaged into the compact 3D printed frame. In addition to optical components, circuits for driving and synchronizing them are also included in the prototype. On the right side, schematic diagram of the prototype is provided. 15 focal planes are floated in real time (60fps) and each focal plane shows the partial image on the DP.

As shown in the Fig. 5, we demonstrate our proof-of-concept HMD prototype to validate its fidelity to generate 15 focal planes. As eyepieces, FTLs released by Optotune (EL10-30-TC-VIS-12D) are used. Single FTL has an 10mm aperture and this model could operate at a speed of 60Hz. We used lens driver 4 of Optotune which is USB-powered current source in order to control the FTL. As the focal power of FTL continuously changes along the input voltage signal, the desired voltage signal of triangular shape is generated by Data Acquisition (DAQ) board from National Instruments.

LBU consists of the 32×64 RGB LED matrix of 3mm pixel pitch from Adafruit and the holographic diffuser with 60° diffusing angle from Edmund Optics. Due to the low fill factor of LED array pixel, the pixelated structure of LED array could be shown through DP. Optical diffuser alleviates the seam effect if it is placed at optimal distance from the LED array since it functions as a Gaussian kernel. We empirically found the optimal spacing to be 3.5mm and measured the Gaussian kernel with standard deviation of 2.2mm. The LED panel vetically scans at 1:16 rates. To display binary images in LBU, we used Arduino DUE microcontroller board. Adafruit industries provide the basic software to display desired images in the LED panel and we modified it

to drive the panel fast. We use an Topfoison TF60010A liquid-crystal display (LCD) panel with a resolution of 2560×1440 pixels for the DP. 8×8 LED pixels and 600×600 LCD pixels are used for display area.

The LBU and FTL should operate in synchronized states to float focal planes at the accurate distance. For synchronization, the external trigger signal is created with DAQ board and it guides the timing to modulate LBU. Additional Arduino microcontroller board is used to accept the trigger signal and output LBU driving signal.

4.2 Experimental results

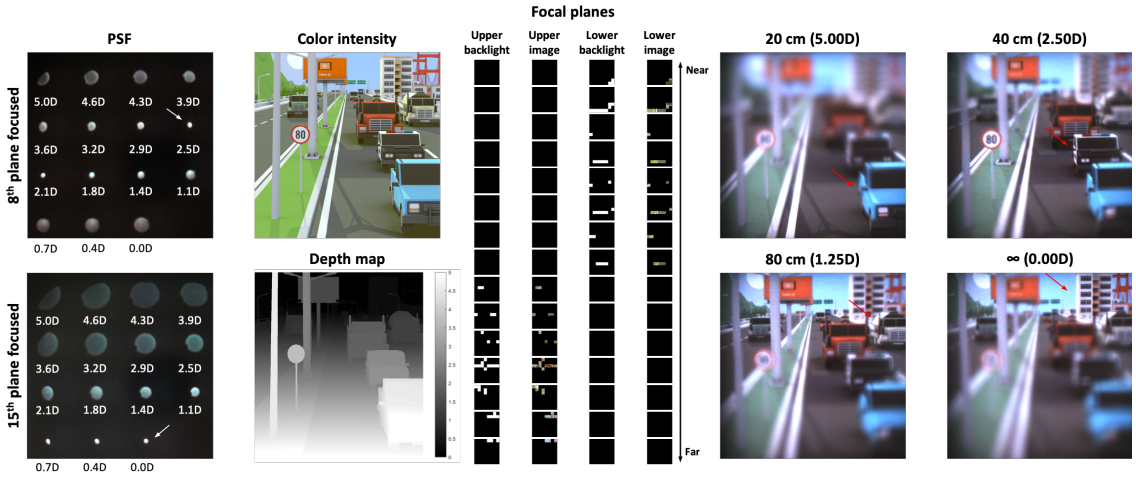

Figure 6. Photographs of experimental results. On the left side, point-spread functions of our prototype are presented for different focal settings, denoted by white arrows. Each point in the figure represents the different focal plane. The point on the upper left is the nearest from the camera and lower right point is the farthest. On the right side, the images are captured for different distances on which the camera focuses with respect to RGBD contents (Source image courtesy: "SimplePolyUrban", www.cgtrader.com). It is observed that distinct object appears to be focused in each image. As shown in the middle, rendered volumetric scenes are composed of 15 focal planes which is generated via our proposed strategy

Figure 6 presents the overall experimental results looking through our prototype. We measured point-spread functions (PSFs) which consists of multiple points located at distinct focal planes in order to evaluate the practical performance for floating focal planes of our prototype. In both PSF images, upper-left points are floated in the 1st focal plane (20cm, 5.0D). For the top image, the camera focuses on the point in the 8th focal plane (40cm, 2.5D) and the point in the 15th focal plane (optical infinity) for the bottom image. Note that the farther away from the focused point in the image, the blur disk diameter gradually increases. We also provide results for computer-generated RGBD contents. For comparison, ground truth images of color intensity and depth map for dioptric unit are presented. The synthesized three-dimensional scenes by our prototype at four distances (20cm, 40cm, 80cm and optical infinity) are shown in the Fig. 6. Focused objects in the images are denoted with red arrows. The blue car object is focused when the camera focuses on the distance of 20cm, and the police car, white truck and the apartment object are focused on the distance of 40cm, 80cm and optical infinity, respectively. It is demonstrated that our prototype supports accommodation cues over the extended depth of field ranging from 20cm to optical infinity.

5. CONCLUSION

In this study, we propose novel type of HMD supporting 15 focal planes with compact form factor. Our tomographic HMD concept uses three main optical components of low-resolution backlight (LED array), display panel (LCD) and focus-tunable lens. Although undesirable seam effect arises due to the usage of backlight with low fill

factor, we resolve it benefiting from optical diffuser which functions as Gaussian kernel. Furthermore, we optimize distance value of unit voxel to mitigate depth distortion within the voxel. Since commercially-available LED array at reasonable prices adopts vertical-scanning method, we also propose the novel strategy of temporally-splitting backlight frame to maximize the focal plane generation capability. In addition to increasing the number of focal planes, we demonstrate that proposed method shows better performance in terms of motion blur and depth distortion against primitive method which applies slight phase difference. In conclusion, we present our proof-of-concept prototype refreshed at 60Hz and synthesizing three-dimensional scenes with 15 focal planes in practice. Photographs of experimental results are also shown to verify the feasibility of our concept. We believe our tomographic HMD could inspire innovative methodologies for virtual reality HMDs.

ACKNOWLEDGMENTS

This work was supported by Institute for Information & Communications Technology Promotion (IITP) grant funded by the Korea government (MSIT) (No. 2017-0-00787, Development of vision assistant HMD and contents for the legally blind and low visions).

REFERENCES

[1] Shibata, T., Kim, J., Hoffman, D. M., and Banks, M. S., "The zone of comfort: predicting visual discomfort with stereo displays," *Journal of Vision* **11**(8), 11–11 (2011).

[2] Hoffman, D. M., Girshick, A. R., Akeley, K., and Banks, M. S., "Vergence-accommodation conflicts hinder visual performance and cause visual fatigue," *Journal of Vision* **8**(3), 33–33 (2008).

[3] Lambooij, M., Fortuin, M., Heynderickx, I., and IJsselsteijn, W., "Visual discomfort and visual fatigue of stereoscopic displays: A review," *Journal of Imaging Science and Technology* **53**(3), 30201–1 (2009).

[4] Rolland, J. P., Krueger, M. W., and Goon, A. A., "Dynamic focusing in head-mounted displays," in [*Stereoscopic Displays and Virtual Reality Systems VI*], **3639**, 463–471, International Society for Optics and Photonics (1999).

[5] MacKenzie, K. J., Hoffman, D. M., and Watt, S. J., "Accommodation to multiple-focal-plane displays: Implications for improving stereoscopic displays and for accommodation control," *Journal of vision* **10**(8), 22–22 (2010).

[6] Hu, X. and Hua, H., "High-resolution optical see-through multi-focal-plane head-mounted display using freeform optics," *Optics express* **22**(11), 13896–13903 (2014).

[7] Llull, P., Bedard, N., Wu, W., Tosic, I., Berkner, K., and Balram, N., "Design and optimization of a near-eye multifocal display system for augmented reality," in [*Propagation through and Characterization of Distributed Volume Turbulence and Atmospheric Phenomena*], JTH3A–5, Optical Society of America (2015).

[8] Akeley, K., Watt, S. J., Girshick, A. R., and Banks, M. S., "A stereo display prototype with multiple focal distances," in [*ACM transactions on graphics (TOG)*], **23**(3), 804–813, ACM (2004).

[9] Lee, S., Jo, Y., Yoo, D., Cho, J., Lee, D., and Lee, B., "Tomoreal: Tomographic displays," *arXiv preprint arXiv:1804.04619* (2018).

[10] Park, J.-H., Hong, K., and Lee, B., "Recent progress in three-dimensional information processing based on integral imaging," *Applied Optics* **48**(34), H77–H94 (2009).

[11] Lee, C.-K., Park, S.-G., Moon, S., and Lee, B., "Viewing zone duplication of multi-projection 3d display system using uniaxial crystal," *Optics express* **24**(8), 8458–8470 (2016).

[12] Huang, F.-C., Chen, K., and Wetzstein, G., "The light field stereoscope: immersive computer graphics via factored near-eye light field displays with focus cues," *ACM Transactions on Graphics (TOG)* **34**(4), 60 (2015).

[13] Lee, S., Jang, C., Moon, S., Cho, J., and Lee, B., "Additive light field displays: realization of augmented reality with holographic optical elements," *ACM Transactions on Graphics (TOG)* **35**(4), 60 (2016).

[14] Moon, S., Lee, C.-K., Lee, D., Jang, C., and Lee, B., "Layered display with accommodation cue using scattering polarizers," *IEEE Journal of Selected Topics in Signal Processing* **11**(7), 1223–1231 (2017).

[15] Kim, D., Lee, S., Moon, S., Cho, J., Jo, Y., and Lee, B., "Hybrid multi-layer displays providing accommodation cues," *Optics Express* **26**(13), 17170–17184 (2018).

[16] Yeom, H.-J., Kim, H.-J., Kim, S.-B., Zhang, H., Li, B., Ji, Y.-M., Kim, S.-H., and Park, J.-H., "3d holographic head mounted display using holographic optical elements with astigmatism aberration compensation," *Optics express* **23**(25), 32025–32034 (2015).

[17] Maimone, A., Georgiou, A., and Kollin, J. S., "Holographic near-eye displays for virtual and augmented reality," *ACM Transactions on Graphics (TOG)* **36**(4), 85 (2017).

[18] Jang, C., Bang, K., Li, G., and Lee, B., "Holographic near-eye display with expanded eye-box," in [*SIGGRAPH Asia 2018 Technical Papers*], 195, ACM (2018).

[19] Lee, S., Cho, J., Lee, B., Jo, Y., Jang, C., Kim, D., and Lee, B., "Foveated retinal optimization for see-through near-eye multi-layer displays," *IEEE Access* **6**, 2170–2180 (2018).

[20] Narain, R., Albert, R. A., Bulbul, A., Ward, G. J., Banks, M. S., and O'Brien, J. F., "Optimal presentation of imagery with focus cues on multi-plane displays," *ACM Transactions on Graphics (TOG)* **34**(4), 59 (2015).

[21] Xiao, L., Kaplanyan, A., Fix, A., Chapman, M., and Lanman, D., "Deepfocus: learned image synthesis for computational displays," in [*SIGGRAPH Asia 2018 Technical Papers*], 200, ACM (2018).

[22] Rathinavel, K., Wang, H., Blate, A., and Fuchs, H., "An extended depth-at-field volumetric near-eye augmented reality display," *IEEE transactions on visualization and computer graphics* **24**(11), 2857–2866 (2018).

[23] Butler, D. J., Wulff, J., Stanley, G. B., and Black, M. J., "A naturalistic open source movie for optical flow evaluation," in [*European Conference on Computer Vision*], 611–625, Springer (2012).

[24] Chakravarthula, P., Dunn, D., Akşit, K., and Fuchs, H., "Focusar: Auto-focus augmented reality eyeglasses for both real world and virtual imagery," *IEEE transactions on visualization and computer graphics* **24**(11), 2906–2916 (2018).